

## An Analysis of the Conditional Instability of the Tropical Atmosphere

EARLE WILLIAMS AND NILTON RENNO

*Center for Meteorology and Physical Oceanography, Department of Earth, Atmospheric and Planetary Sciences, Massachusetts Institute of Technology, Cambridge, Massachusetts*

(Manuscript received 2 October 1991, in final form 29 April 1992)

### ABSTRACT

The ice phase is included in thermodynamic calculations of convective available potential energy (CAPE) for a large number of soundings in the tropical atmosphere, at both land and ocean stations. It is found that the positive-buoyancy contribution to CAPE resulting from the latent heat of fusion more than offsets the negative-buoyancy contribution due to water loading in the reversible thermodynamic process. The departure from moist neutrality in much of the tropical atmosphere exhibits a threshold in boundary-layer wet-bulb potential temperature of 22°–23°C. The corresponding sea surface temperature is approximately 26°C, close to the empirical threshold for hurricane formation, which suggests that conditional instability plays an important role in the latter phenomenon. The simultaneous presence of finite CAPE and infrequent deep convection in the tropics is tentatively attributed to the convective inhibition energy (CINE) and to the mixing process that destroys positive buoyancy in incipient cloud parcels.

### 1. Introduction

This study is concerned with the energy available for convection in the tropical atmosphere. Our interest in this topic grew out of efforts to understand the role of deep tropical convection in the global electrical circuit (Williams et al. 1992; Williams 1992) and the reasons for the order-of-magnitude differences in lightning activity between land and ocean (Orville and Henderson 1986). The global circuit studies support a fundamental role for ice in accounting for cloud electrical behavior. While electricity is emphasized less in the present study, ice continues to hold center stage.

Calculations of convective available potential energy (CAPE) for many tropical stations in section 3 are intended to evaluate the effect of freezing on parcel buoyancy in reversible ascent, for comparison with the effect of water loading alone in currently popular calculations based on reversible thermodynamics. CAPE is shown to be linearly correlated with boundary-layer moist entropy, and section 4 is concerned with the global distribution of wet-bulb potential temperature, a direct measure of moist entropy. The large areas of stored energy in the tropics pose questions about the release of conditional instability that are examined in section 5.

### 2. Data sources

Assessments of conditional instability in this study were made possible by the availability of a large number of soundings in a variety of tropical regions. The Atlantic Ocean soundings were obtained from GATE (Global Atlantic Tropical Experiment) from June to September 1974. The soundings from South America were taken in ABLE (Amazon Boundary Layer Experiment) (Garstang et al. 1990), and the Australian soundings were obtained from AMEX (Australian Monsoon Experiment) in January and February of 1987, and in subsequent studies in Darwin in 1988–1990 as part of DUNDEE (Down Under Doppler Electrical Experiment) (Williams et al. 1992; Rutledge et al. 1992). Additional thermodynamic data were also available from the Line Islands experiment (Zipser and Taylor 1968) over the central Pacific Ocean.

This study has also made use of Doppler radar data on tropical convection collected with the Massachusetts Institute of Technology's transportable C-band radar during two wet seasons in Darwin, Australia (12°S).

### 3. The evaluation of parcel buoyancy and CAPE

#### a. The effect of thermodynamic process

The energy realized according to parcel theory when conditional instability is released is CAPE, a quantity first conceptualized by Margules (1905), but named by Moncrieff and Miller (1976)

$$\text{CAPE} = \int_{\text{LFC}}^{\text{LNB}} (T_{vp} - T_{va}) R_d d \ln P, \quad (1)$$

*Corresponding author address:* Dr. Earle Williams, Center for Meteorology and Physical Oceanography, Massachusetts Institute of Technology, Department of Earth, Atmospheric and Planetary Sciences, Cambridge, MA 02139.

where LFC is the level of free convection, LNB is the level of neutral buoyancy, and  $T_{vp}$  and  $T_{va}$  are the virtual temperatures of the parcel and the environment, respectively. Here,  $R_d$  is the gas constant for dry air, and  $P$  is pressure. CAPE is the integrated effect of the rather modest positive buoyancy (a few degrees Celsius at most) of the rising undiluted parcel relative to its environment. Several different procedures have been suggested for evaluating CAPE, depending on certain thermodynamic and microphysical assumptions. The choice of procedure is often crucial, because the assumption can affect the parcel buoyancy at the level of 1 K as was shown earlier by Saunders (1957). We shall be concerned here with a comparison of three specific processes: 1) the standard irreversible ("pseudoadiabatic") process, 2) the reversible process, and 3) the reversible process including the ice phase. These three processes are now discussed in turn.

### 1) IRREVERSIBLE OR PSEUDOADIABATIC PROCESS

First formulated by von Bezold in 1888 (see McDonald 1963), this process follows the thermodynamic relation [see Iribarne and Godson (1981), Eq. (85)]

$$C_{pd} \ln T + C_w \int r_w d \ln T - R_d \ln P_d + \frac{r_w L_v}{T} = \text{constant.} \quad (2)$$

Here,  $C_{pd}$  and  $C_w$  are the heat capacities (at constant pressure) of dry air and water vapor, respectively,  $T$  is temperature,  $r_w$  is the mixing ratio of water vapor,  $R_d$  is the gas constant for dry air,  $P_d$  is the partial pressure of dry air, and  $L_v$  is the latent heat of vaporization. In this process, it is assumed that all liquid water condensate is removed from the parcel the instant it appears. This assumption eliminates the need to consider the effects of either water loading or the heat capacity of condensate on the subsequent motion of the parcel. This assumption, however, conflicts with the observation of precipitation formation and the appearance of radar echo at all but the very highest levels in deep tropical convection.

### 2) REVERSIBLE PROCESS

First formulated by Reye in 1864 (see McDonald 1963), this process follows the thermodynamic relation [see Iribarne and Godson (1981), Eq. (80)]

$$(C_{pd} + r_i C_w) \ln T - R_d \ln P_d + \frac{r_w L_v}{T} = \text{constant,} \quad (3)$$

where  $r_i = r_w + r_l$ , the sum of the water vapor and liquid water mixing ratios, respectively. In this process, the assumption made is the other extreme when compared with the aforementioned pseudoadiabatic assumption: as liquid-phase condensate forms, it not only is retained in the parcel, but is carried upward along the parcel's entire trajectory. While the formation and

removal of precipitation are ignored in the reversible process, both the important effects of water loading and heat capacity of the condensate are included. Betts (1982), Emanuel (1988), and Xu and Emanuel (1989) have recently advocated the use of this process in evaluating CAPE in tropical soundings.

### 3) REVERSIBLE PROCESS INCLUDING THE ICE PHASE

Although the significant effects of the latent heat of fusion in parcel buoyancy have long been recognized (Saunders 1957), ice has only rarely (e.g., Chapell and Smith 1975) been included in CAPE calculations. The reasons are attributable to the acknowledged presence of supercooled water (i.e., liquid water condensate) well above the 0°C isotherm with the attendant ambiguity in choice of freezing level for the condensate. In deep tropical convection, which often extends several kilometers above the -40°C isotherm and which exhibits radar echoes at these high levels, there is little doubt that the liquid water condensate eventually freezes, and therefore the freezing process deserves inclusion in the thermodynamics. In situ observation in the tropics at altitudes above the 0°C isotherm disclose the presence of ice particles in deep convection (Gamache 1990). Perhaps the most dramatic evidence for ice in deep tropical convection is the prodigious lightning activity that is believed to be caused by collisions between graupel and small ice particles (Williams 1989).

The isentropic quantity in the reversible process including ice follows Eq. (3) for parcels warmer than the freezing temperature. For parcels attaining the temperature at which freezing is initiated,  $T_f$ , isobaric freezing is assumed with an increase in parcel temperature caused by both the latent heat of freezing and the deposition of water vapor (due to the decrease in saturation pressure). The temperature increase is given by [see Iribarne and Godson (1981), Eq. (94)]

$$\Delta T = \frac{L_f r_l + L_s r_w (1 - e_i / e_w)}{C_{pt} + (r_i L_s / R_v T^2)}, \quad (4)$$

where  $L_f$  and  $L_s$  are the latent heats of freezing and sublimation, respectively. The liquid water mixing ratio is  $r_l$ , and  $r_i$  is the saturation mixing ratio over ice. Saturation vapor pressure with respect to ice and water are  $e_i$  and  $e_w$ , respectively. The total heat capacity  $C_{pt}$  has contributions from dry air, water vapor, and ice-phase condensate

$$C_{pt} \approx C_{pd} + r_i C_{pv} + r_s C_i, \quad (5)$$

with

$$r_s(T) \approx r_l + r_w(T) - r_i(T'), \quad (6)$$

and

$$r_w \approx \epsilon \frac{e_w(T)}{p} \quad (7)$$

$$r_i \approx \epsilon \frac{e_i(T')}{p}, \quad (8)$$

where  $\epsilon$  is the ratio of gas constants for dry air and water vapor. The parcel temperature after freezing  $T'$  is elevated  $\Delta T$  relative to the freezing temperature  $T_f$  according to

$$T' = T_f + \Delta T, \quad (9)$$

and the expression for moist entropy after freezing is

$$(C_{pd} + r_i c_i) \ln T - R_d \ln P_d + \frac{r_i L_s}{T} = C_2, \quad (10)$$

where

$$C_2 = (C_{pd} + r_i c_i) \ln T' - R_d \ln P_d + \frac{r_i(T')L_s}{T'}. \quad (11)$$

The effects of the various assumptions in evaluating CAPE are best seen in comparisons of parcel buoyancy with height from a particular tropical sounding following the three thermodynamic procedures just outlined. These comparisons are shown in Fig. 1. The parcel-buoyancy parameter in these calculations is cloud virtual potential temperature (Betts 1982). For the reversible process involving ice, isobaric freezing is assumed at  $-10^\circ\text{C}$  for all calculations in this paper. The irreversible calculation shows significantly more buoyancy than the reversible calculation through most of the troposphere except at upper levels, where the heat capacity of liquid water tends to suppress cooling relative to the condensate-free irreversible process. When ice is included, the buoyancy in the reversible process is significantly enhanced at and above the freezing level.

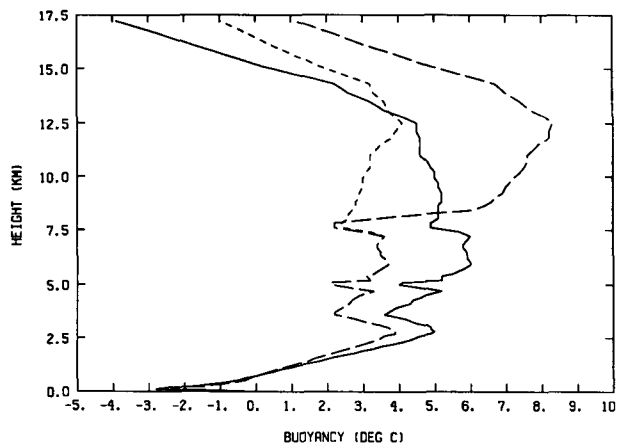


FIG. 1. Parcel buoyancy ( $K$ ) versus height for three thermodynamic processes [pseudoadiabatic (solid line), reversible (short-dashed line), and reversible with ice (long-dashed line)] for a sample tropical sounding from the PRC ship north of Australia. For the reversible-with-ice process, the conversion to ice is initiated at  $T = -10^\circ\text{C}$ , near the 7.5-km altitude.

The buoyancy exceeds that of the process with liquid water because of the latent heat of freezing.

While it is noted that the vertical distribution of buoyancy and CAPE are both affected by the choice of freezing level, the choice is reasonably bounded by  $0^\circ$  and  $-20^\circ\text{C}$ , a temperature interval over which observed ice nuclei are scarce. Since the corresponding interval in height ( $\sim 3$  km) is a modest fraction of the interval over which CAPE has significant contributions in the tropical atmosphere ( $\sim 15$  km), it is apparent that the choice of freezing level is not too crucial. Sensitivity calculations, not shown here, illustrate this point quantitatively.

The effect of parcel buoyancy on CAPE for the three thermodynamic processes is illustrated by the histograms in Fig. 2 for large numbers of sequential soundings in Darwin, Australia, Belem, South America, and from the PRC and *Quadra* ships in AMEX and GATE, respectively. Generally speaking, the effects of condensate loading on the reversible process substantially diminish CAPE relative to the pseudoadiabatic process (consistent with earlier results by Betts 1982; Emanuel 1988; and Xu and Emanuel 1989), but the inclusion of the ice phase in the reversible process moves the CAPE values back to their levels obtained with the standard irreversible process. To a good approximation, the negative buoyancy caused by condensate loading is compensated by the positive buoyancy caused by the latent heat of fusion.

*b. The effect of wet-bulb temperature in the boundary layer*

In all of the calculations of CAPE presented thus far, the thermodynamic properties of the lifted parcel are taken to be those specified by the surface measurements in the available sounding. This procedure may well be unrealistic, but serves to provide upper bounds for CAPE. The importance of this choice may be evaluated, first by considering the change in CAPE affected by a change in wet adiabat of  $1^\circ\text{C}$ . For a typical surface wet-bulb temperature of  $24^\circ\text{C}$ , a  $1^\circ\text{C}$  change in moist adiabat results in a change of CAPE (irreversible process) of about  $1000 \text{ J kg}^{-1}$ , for a parcel excursion from the surface ( $P \approx 1000 \text{ mb}$ ) to the parcel equilibrium level. This value is already of the same order as CAPE values in the tropical atmosphere (recall Fig. 2); one degree has a substantial effect.

To determine the sensitivity of CAPE to the originating height of the hypothetical boundary-layer parcel, it is necessary to know the lapse rate of wet-bulb potential temperature  $\theta_w$  in the lower tropical atmosphere. Figure 3 shows a compilation of  $\theta_w$  versus height for Darwin, Australia. Examination of such plots for a large number of tropical stations (see Table 1) shows that  $\theta_w$  generally decreases with height, at a rate of  $0.15^\circ\text{--}0.25^\circ\text{C} (100 \text{ m})^{-1}$ . Combined with the earlier findings (and the results to be discussed in Table 1), this result

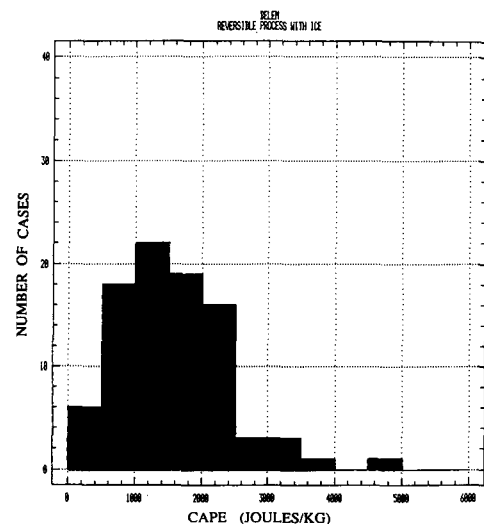
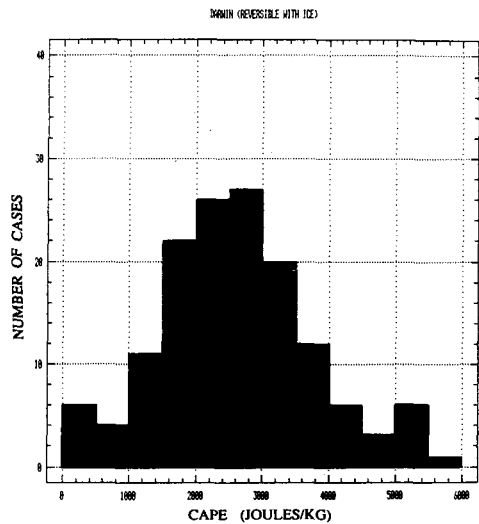
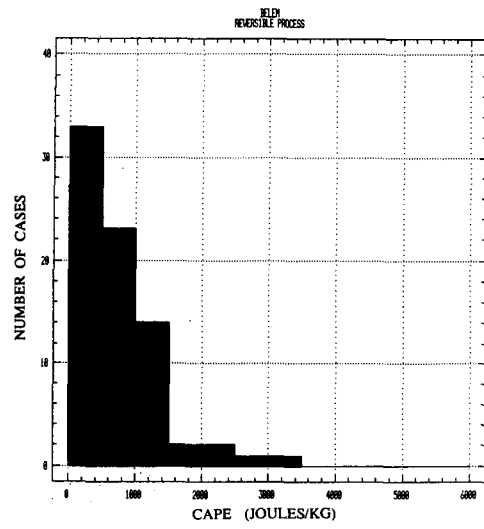
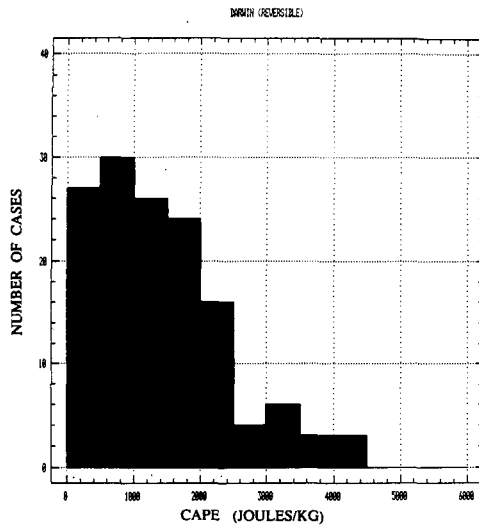
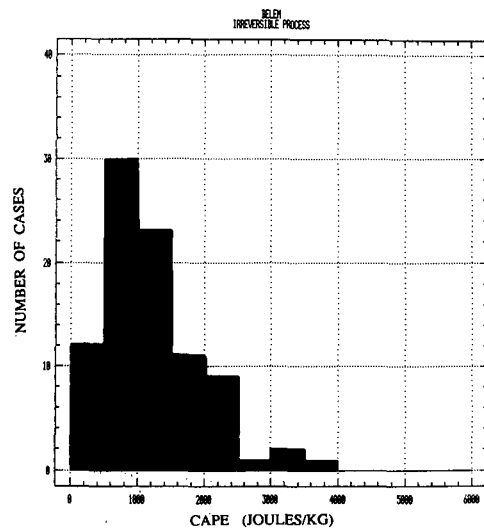
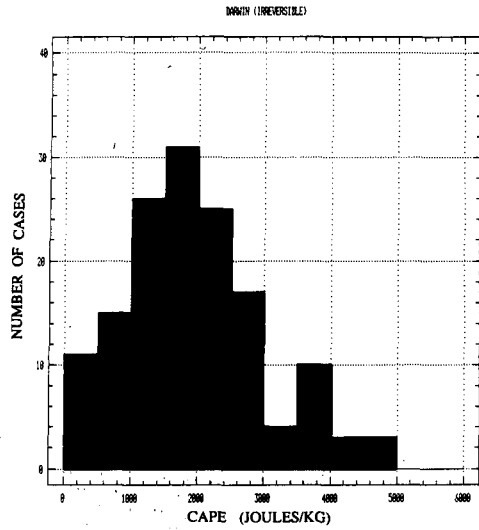


FIG. 2a. CAPE histograms (three methods) for soundings in Darwin, Australia.

FIG. 2b. CAPE histograms (three methods) for soundings in Belém, South America.

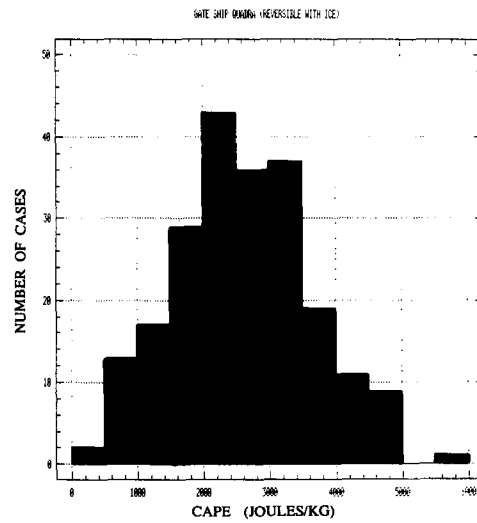
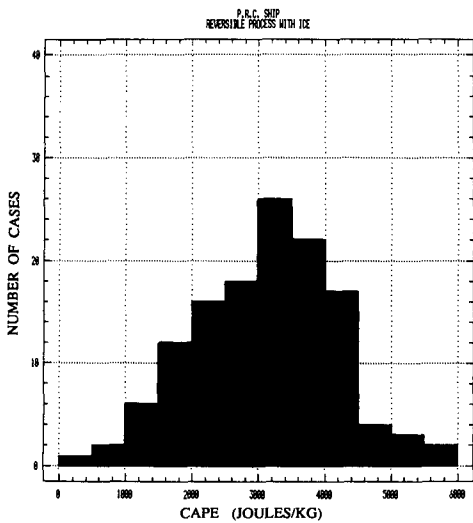
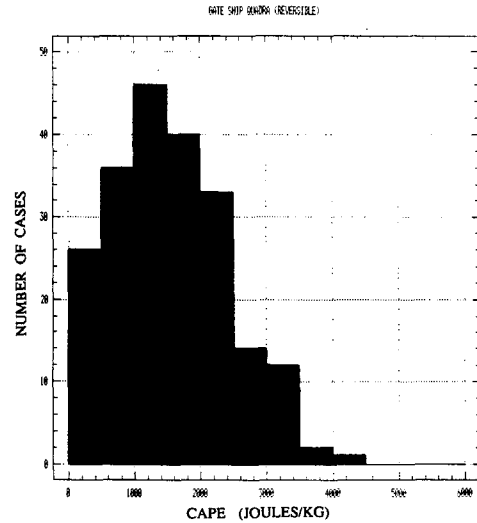
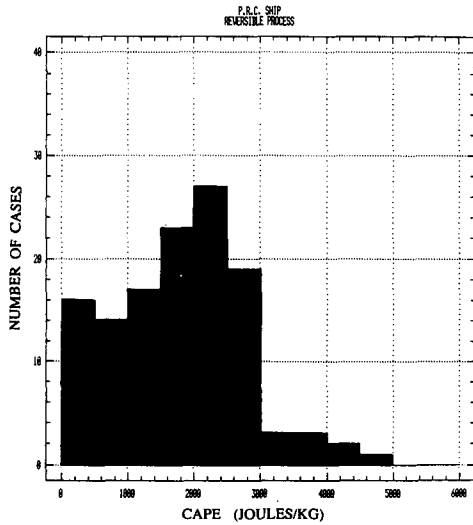
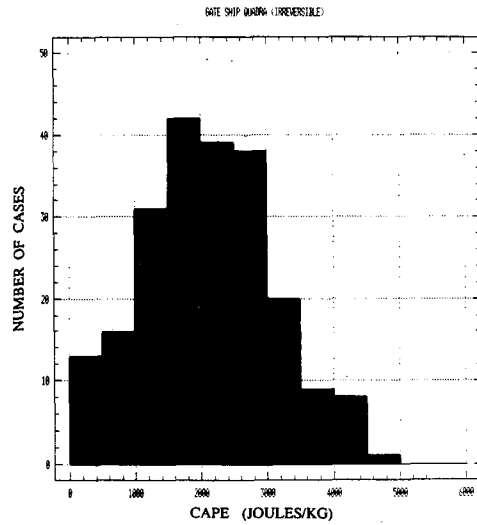
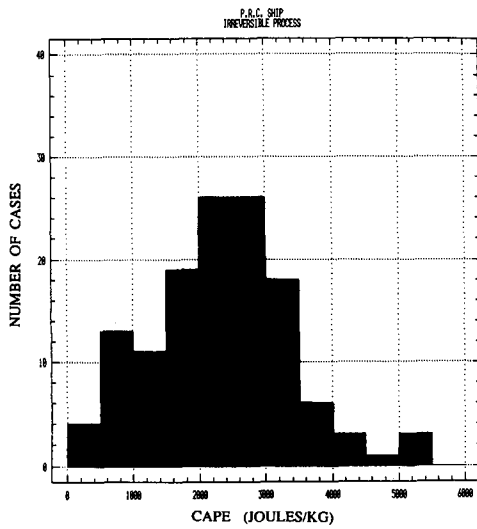


FIG. 2c. CAPE histograms (three methods) for soundings from the PRC ship in AMEX.

FIG. 2d. CAPE histograms (three methods) for soundings from the ship *Quadra* in GATE.

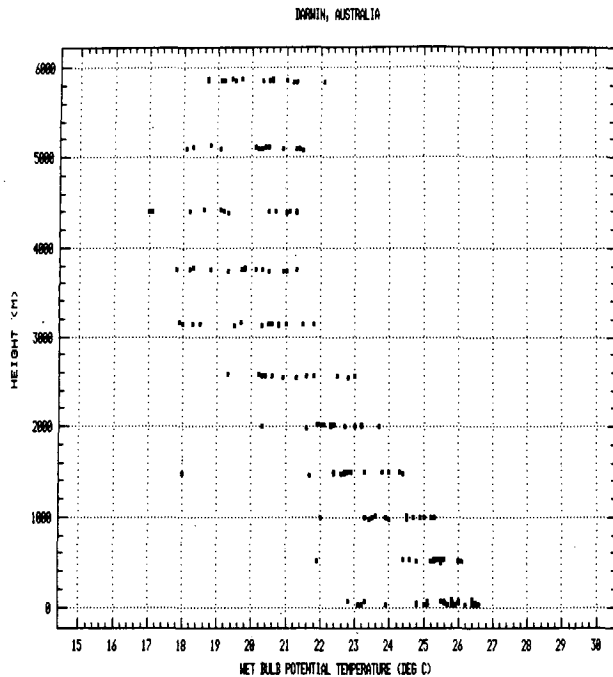


FIG. 3. Wet-bulb potential temperature versus height for several Darwin soundings.

shows a diminishment in computed CAPE of  $150\text{--}250 \text{ J kg}^{-1}$  for every 100 m of initial height for the ascending parcel.

To what extent is CAPE determined by the wet-bulb potential temperature of boundary-layer air? Clearly, if tropical soundings were invariable except for changes in the boundary-layer air, then CAPE, following (1), is entirely dependent on the  $\theta_w$  of the boundary-layer air, and should increase approximately linearly with the latter quantity as the wet-bulb adiabat translates away from the sounding. As a further test of this condition, scatterplots of CAPE versus surface values of  $\theta_w$  were assembled for tropical stations listed in Table 1. Selected examples using the pseudoadiabatic process [Eq. (2)] from Darwin, Australia; Belém, South America; the Atlantic Ocean in GATE; and for Ponape in the western Pacific Ocean are shown in Fig. 4. In most cases, CAPE is seen to increase approximately linearly with  $\theta_w$ , with correlation coefficients of 0.8–0.9. The value of  $\theta_w$  at which CAPE vanishes is called the zero-CAPE intercept  $\theta_{wc}$ . Values for these intercepts are listed in Table 1 and are seen to be narrowly distributed around  $22^\circ\text{--}23^\circ\text{C}$  for stations around the globe. From a statistical standpoint, a knowledge of surface wet-bulb temperature allows the empirical prediction of CAPE to within about 25%. Consistent with the findings in the earlier section, the zero-CAPE intercepts are slightly dependent on the thermodynamic process; Table 1 summarizes slopes and intercepts for all stations analyzed and for each of three thermodynamic processes discussed earlier. The mean intercept when ice is included is about  $0.3^\circ\text{C}$  larger than the

mean intercept with the standard irreversible calculation. The mean slope ( $\text{J kg}^{-1} \text{ }^\circ\text{C}^{-1}$ ) is about 5% greater when ice is included.

Comparisons between GATE and the other stations in Table 1 show that the zero-CAPE intercepts are slightly, but systematically, smaller in South America and the Atlantic than in the warmer western Pacific.

### c. CAPE and the validity of parcel theory in deep tropical convection

For lossless conversion of potential energy to kinetic energy, the maximum upward velocity achieved by a parcel at level  $i$ , acted on by buoyancy forces alone, is given by

$$w = [2(\text{CAPE}_i)]^{1/2} \quad (12)$$

where  $\text{CAPE}_i$  is the integrated CAPE from the level of free convection to level  $i$ . This result is an important observational constraint on the validity of parcel theory (e.g., Bluestein et al. 1989). Direct observations with Doppler range-height indicator (RHI) scans on nearby hot towers in Darwin, Australia, (Williams et al. 1992) showed velocities that were significantly smaller than values predicted by (12), regardless of the method chosen for CAPE calculation, including the choice of height of parcel origination. For example, for a CAPE value of  $1000 \text{ J kg}^{-1}$ , a modest value given the results shown in Figs. 2 and 4, the corresponding vertical velocity following parcel theory is  $45 \text{ m s}^{-1}$ . In two wet seasons of observations, a value this large was recorded only once. Most vertical velocities were in the range of  $10\text{--}25 \text{ m s}^{-1}$ . The Doppler RHIs also indicated rather narrow tower widths ( $\sim 5 \text{ km}$ ) aloft with significant lateral inflow, suggesting an important role for entrainment and consequent departures from undilute parcel ascent. Studies by Kingsmill et al. (1989) also provide evidence for departures from parcel theory in deep convection.

In light of this evidence for a significant failure of parcel theory, the choice of method for CAPE calculations is generally unconstrained by the observations of vertical air velocity.

## 4. Global climatology of wet-bulb potential temperature

The reasonably well-defined relationships (shown in section 3b) between CAPE and the wet-bulb potential temperature of boundary-layer air, over both land and ocean in the tropics, suggests that the global distribution of surface  $\theta_w$  will be a reliable indicator of the distribution of energy stored in the tropical atmosphere. Monthly mean values of wet-bulb temperature for tropical land stations were calculated from tabulated temperatures (Meteorological Office 1965) and vapor pressures (NCDC 1988) and from a recently published climatology of wet-bulb temperature (International Station Meteorological Climate Summary 1990). The wet-bulb temperatures were subsequently corrected for

TABLE 1. Summary of zero-CAPE intercepts of wet-bulb potential temperature  $\theta_{wc}$  in degrees Celsius and slopes of best fit [ $d(\text{CAPE})/d\theta_w$  ( $\text{J kg}^{-1} \text{ } ^\circ\text{C}^{-1}$ )] for analyzed tropical soundings.

Station	Latitude	Longitude	Irreversible	Reversible	Reversible with ice
Australia—AMEX					
Darwin	12°S	131°E	23.1 (1090)	23.6 (1030)	22.8 (1260)
Gove	12°S	137°E	23.0 (1150)	23.4 (1110)	22.6 (1310)
Thursday Island	11°S	142°E	23.2 (1210)	23.7 (1200)	22.9 (1360)
Broome	18°S	122°E	23.4 (1190)	23.8 (1110)	22.8 (1090)
Hall's Creek	18°S	128°E	22.9 (870)	23.3 (760)	22.8 (1090)
Townsville	19°S	147°E	21.9 (780)	22.4 (710)	21.8 (940)
Willis Island	16°S	150°E	22.0 (940)	22.5 (920)	21.7 (1050)
Mount Isa	21°S	140°E	21.7 (580)	22.0 (450)	21.7 (730)
Weipa	13°S	142°E	23.3 (1170)	23.8 (1170)	22.9 (1300)
Burketown	18°S	140°E	23.0 (1020)	23.5 (980)	22.7 (1170)
Borroloola	16°S	136°E	23.0 (1170)	23.8 (1120)	23.0 (1320)
PRC ship	11°S	139°E	23.4 (1300)	23.9 (1290)	23.0 (1380)
South America—ABLE					
Belém	1.5°S	49°W	22.5 (790)	23.1 (682)	22.0 (819)
Boa Vista	3.2°S	61°W	22.6 (940)	23.1 (860)	22.3 (1020)
Tabatinga	4.1°S	70°W	22.9 (1000)	23.4 (932)	22.8 (1180)
Vilhena	13°S	60°W	21.5 (480)	22.3 (397)	21.2 (520)
Alta Floresta	12°S	55°W	22.3 (760)	22.8 (616)	22.2 (920)
Embrapa	3.0°S	60°W	21.2 (613)	21.7 (534)	20.5 (560)
Atlantic Ocean—GATE					
Researcher ship	7°N	23°W	21.3 (860)	21.8 (730)	21.1 (990)
<i>Quadra</i>	9°N	22°W	21.7 (990)	22.2 (900)	21.5 (1090)
<i>Onversaagd</i>	15°N	54°W	21.1 (830)	21.7 (760)	20.9 (950)
Ascension Island	8°S	14°W	19.6 (380)	19.5 (260)	19.6 (470)
Barbados	13°N	59°W	21.6 (1050)	22.0 (950)	21.5 (1180)
Trinidad	11°N	61°W	21.5 (980)	22.0 (900)	22.2 (1080)
Pacific Ocean—GATE					
Ponape	7°N	158°E	22.4 (1170)	22.9 (1150)	22.1 (1270)
Africa—GATE					
Malakai	10°N	32°E	22.6 (1020)	23.1 (960)	22.5 (1130)
Port Sudan	20°N	37°E	23.6 (1200)	24.0 (1150)	23.4 (1300)

mean station pressure to determine  $\theta_w$ . Over ocean regions, tabulated values of sea surface temperature and air-sea temperature differences (Bottomley et al. 1990) were used to determine boundary-layer temperature, and a fixed relative humidity of 80% was assumed (Riehl 1954) in calculating  $\theta_w$  values. Subsequent calculations of the relative humidity in the boundary layer over the oceans using data from Bottomley et al. (1990) showed that the latter assumption was quite accurate. Climatological maps of  $\theta_w$  for January and July are shown in Fig. 5, where 1°C contours have been used.

Both January and July maps show three well-defined maxima (25°C and larger) in  $\theta_w$  associated with tropical continental zones (the Americas, Africa, and the maritime continent). These elevated values are largely attributable to the effects of temperature; the land surface (solid, immobile, with low heat capacity) is more strongly heated than the ocean. It should be noted,

however, that the surface mixing ratio over tropical continental zones is also slightly elevated relative to the adjacent oceans (Newell et al. 1972), thereby contributing to elevated values of moist entropy over the continents.

The central oceans (both Atlantic and Pacific) exhibit  $\theta_w$  values close to 22°–23°C, the zero-CAPE intercept in the scatterplots shown in Fig. 4 and tabulated for a larger number of stations in Table 1. Oceanic regions noted for tropical cyclone formation—the western regions of the tropical Atlantic and Pacific oceans, the Bay of Bengal, and the eastern Pacific off Mexico—all exhibit  $\theta_w$  values that are greater than the zero-CAPE intercept, but significantly less than the land values. The comparatively smaller values of CAPE in the GATE soundings are consistent with the small updrafts recorded in that experiment (Lemone and Zipser 1980).

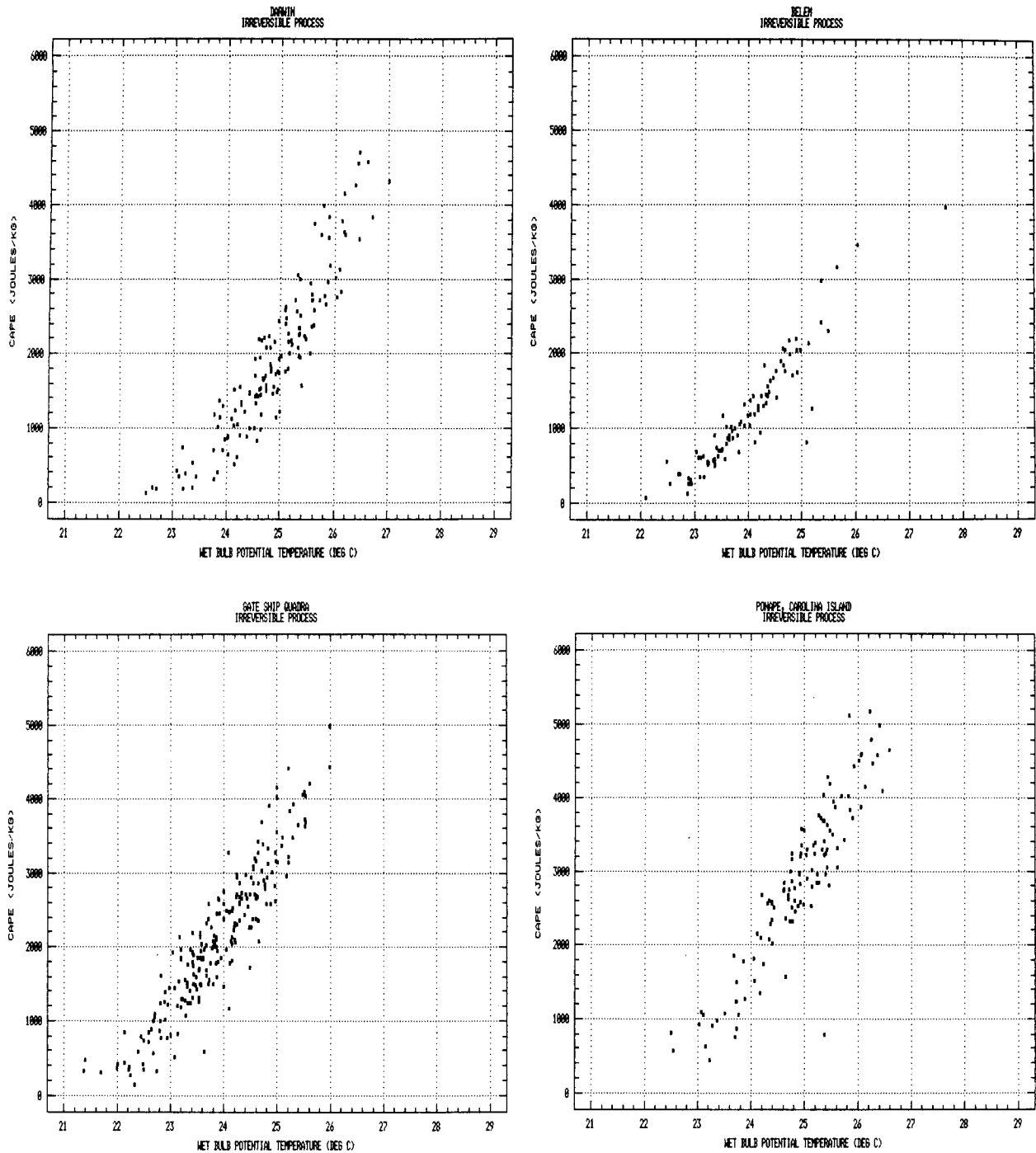


FIG. 4. CAPE versus  $\theta_w$  for (a) Darwin, Australia; (b) Belem, South America; (c) the *Quadra* ship (GATE) in the Atlantic Ocean; and (d) Ponape in the western Pacific Ocean.

The climatology in Fig. 5 shows considerable agreement with global maps of deep cloudiness (Suskind et al. 1984; Markson 1986), outgoing longwave radiation (Bess et al. 1989), cloud albedo (Harrison et al. 1990), high-level cirrus cloud (Chiou et al. 1990), upper-level water vapor (Bannon and Steele 1957; Newell

et al. 1972), and the distribution of global lightning (Kotaki and Katoh 1983; Orville and Henderson 1986). This general agreement supports the idea that CAPE is present in regions of deep convection and plays an important role in promoting ice particles to the upper troposphere.



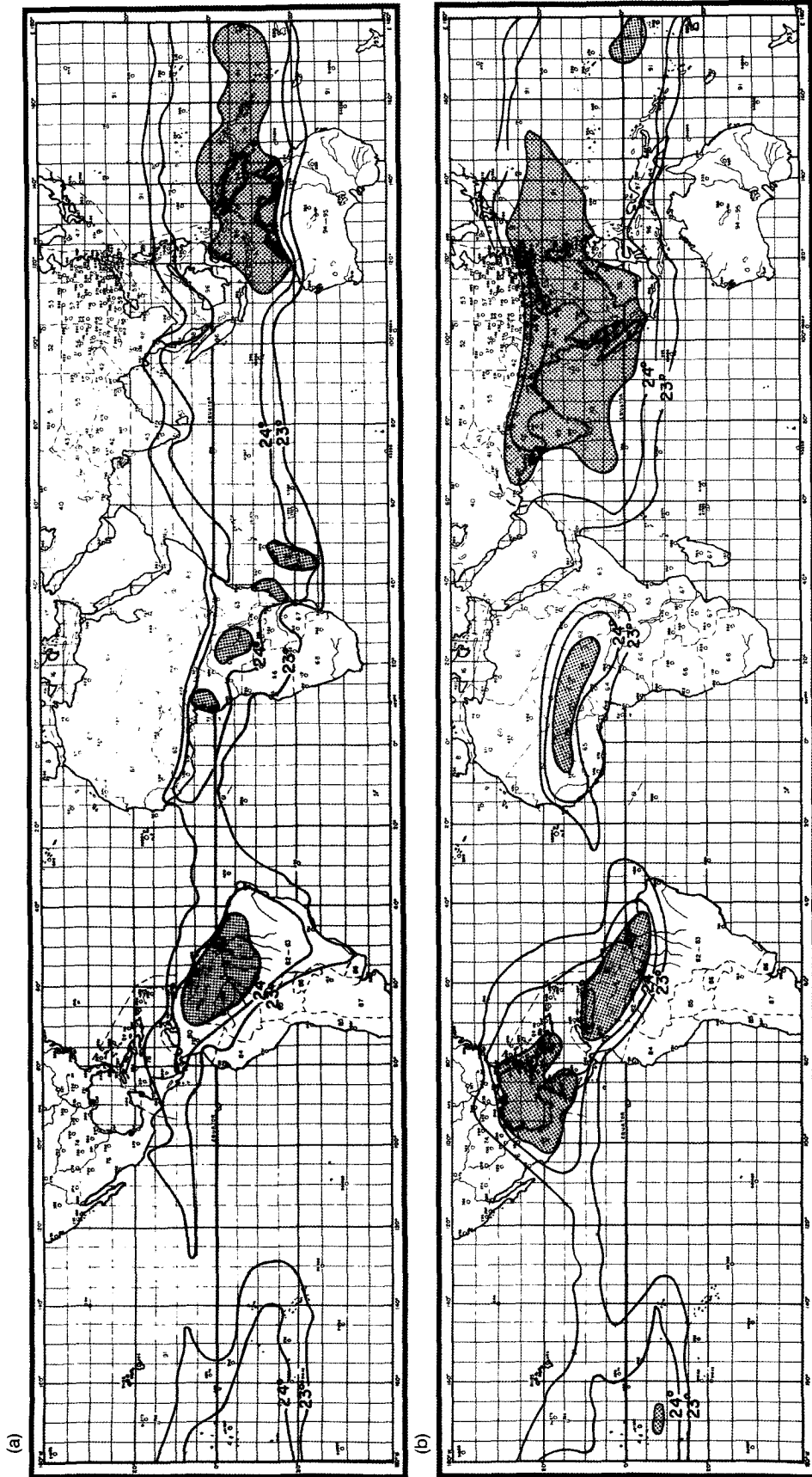


FIG. 5. Global climatology of mean maximum wet-bulb potential temperature for (a) January and (b) July.

## 5. The areal release of conditional instability

The calculations presented thus far indicate that stored energy of the order of  $1000 \text{ J kg}^{-1}$  of air are present over large areas of the tropics, over land areas, and over the warmer parts of the oceans as well. Further calculations, shown in Fig. 6, show that CAPE is sustained throughout the course of a day as well. Despite this widespread availability of energy for instability, observations show that deep convection breaks out over a relatively small area. Figure 7 shows a histogram of the *maximum* fractional area covered by radar echoes (15-dBZ threshold) over the course of 47 days of the wet season in Darwin, Australia. The geometric mean value for maximum fractional area is only 7%. The largest values in this histogram ( $\sim 40\%$ ) are associated with monsoonal convection when CAPE values are at their minimum level for the wet season.

In search of possible barriers to the initiation of conditional instability, the convective inhibition energy (CINE) was examined for the same set of tropical soundings used for CAPE calculations. CINE is represented by the negative area on the tephigram at low levels and is defined by

$$\text{CINE} = \int_{\text{sfc}}^{\text{LFC}} (T_{vp} - T_{va}) R_d d(\ln P). \quad (13)$$

Here,  $T_{vp}$  and  $T_{va}$  are the ambient virtual temperatures of the environment and cloud parcel, respectively.

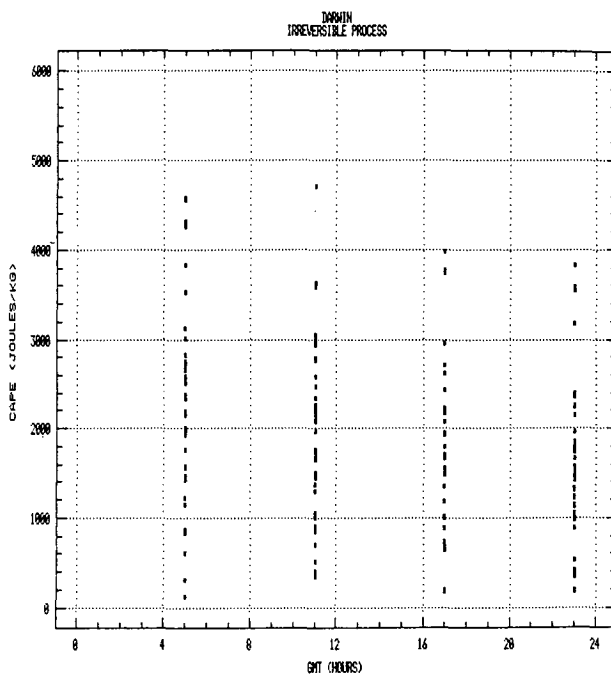


FIG. 6. Diurnal variation of CAPE for Darwin, Australia (all AMEX soundings).

Histograms of CINE values for four tropical stations are shown in Figs. 8a–d. The values range from 0 to about  $200 \text{ J kg}^{-1}$  with mean values of about  $20 \text{ J kg}^{-1}$ .

The mean values are small (relative to CAPE values), but are by no means negligible. According to (12), in order to overcome a negative area of  $20 \text{ J kg}^{-1}$ , a parcel velocity of  $6.3 \text{ m s}^{-1}$  is required. Such a velocity is far in the tail of velocity distributions associated with boundary-layer thermals (Lenschow and Stephens 1980; Raymond and Wilkening 1982). This result suggests that CINE can frequently present a significant barrier to the release of conditional instability in the tropics.

Figures 8a–d also show that on other occasions, the CINE values are essentially zero, and no capping inversions are present. It is possible that conventional radiosoundings are too coarse a tool for resolving small CINE values. If CINE is essentially zero, however, alternative barriers must be examined to explain the large reservoir of CAPE in the tropical atmosphere. One possibility, not examined in this study, is the entrainment process itself, which may render neutral buoyancy to small cloudy parcels in their early stages of formation.

## 6. Discussion

### a. How should CAPE be calculated for tropical soundings?

CAPE is unambiguously determinable only within the confines of parcel theory, and a number of observations show that parcel theory is an inaccurate approximation. Furthermore, the parcel theory processes of reversible and irreversible (pseudoadiabatic) displacements represent extreme situations in which the precipitation efficiency is either 0% or 100%, respectively. Given these discrepancies between theory and reality, how is CAPE most accurately calculated?

Betts (1982), Emanuel (1988, 1989), and Xu and Emanuel (1989) all advocate the use of reversible thermodynamics in the evaluation of conditional instability, and water loading substantially reduces CAPE values in comparison to pseudoadiabatic calculations, as shown clearly in Figs. 1 and 2. In recent years, this result has become a mainstay of the argument that the tropical atmosphere is in a state of moist neutrality. Consistent with the assumptions of reversible displacements and a distinct departure from the pseudoadiabatic assumption, radar observations of deep tropical hot towers provide firm evidence for the lifting of precipitation condensate aloft. Observations also show (Gamache 1990), however, that the condensate above the  $0^\circ\text{C}$  isotherm in deep tropical convection is predominantly ice rather than liquid water. The most dramatic probable manifestation of this ice is the lightning activity over tropical land regions and the warmer areas

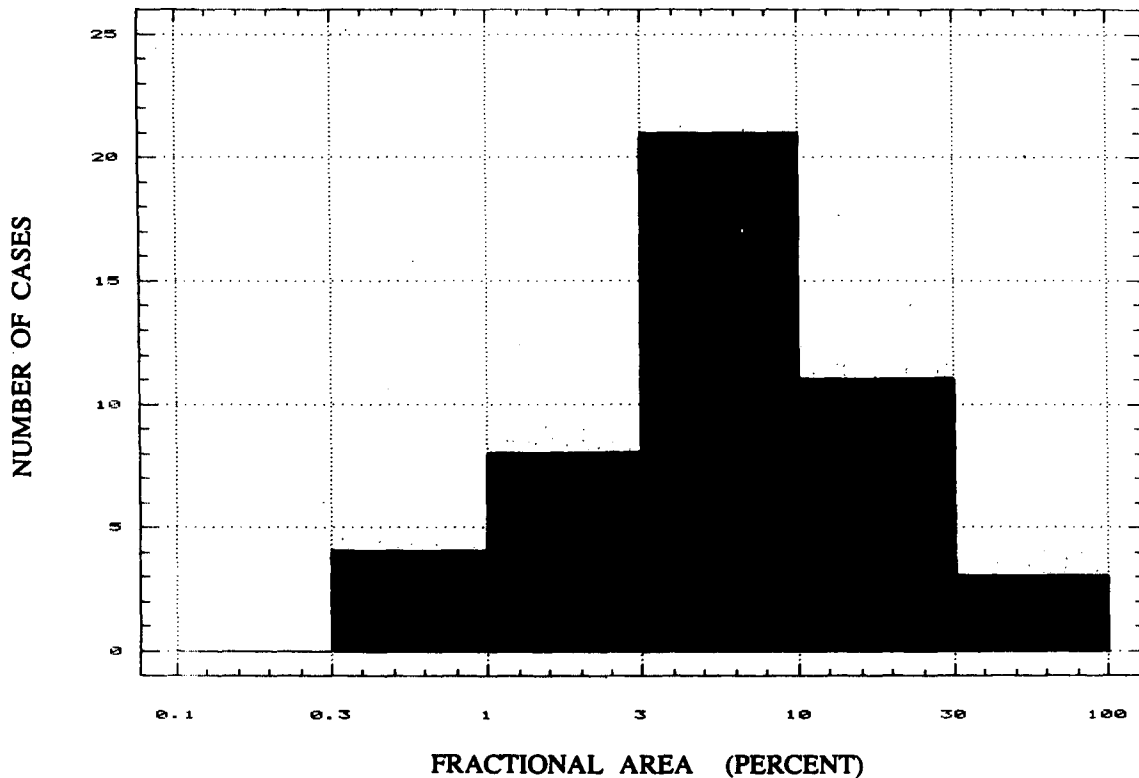


FIG. 7. Histogram of maximum daily fractional area covered by precipitation echoes within the 40 000-km<sup>2</sup> area of radar surveillance during the wet season in Darwin, Australia.

of the oceans (Williams et al. 1991), and there is now considerable evidence that the global electrical circuit is dependent on ice (Williams 1989). When the latent heat of freezing is included in evaluating parcel buoyancy, the results presented here show that CAPE values are as large or larger than values obtained by the pseudoadiabatic assumption, as shown in Fig. 2. The positive buoyancy due to the ice phase more than offsets the water loading, also shown in Fig. 2. This result was really shown earlier by Saunders (1957), but the acknowledged persistence of supercooled water, the ambiguity of selection of freezing level, together with the complication of the phase change in the analytical treatment, have discouraged most efforts to include the ice phase in thermodynamic calculations.

The predictions of parcel theory when ice is included show a pronounced increase in buoyancy with height above the level of freezing, as was shown in Fig. 1. A likely manifestation of this extra buoyancy in continental convection are the observations of enhanced horizontal convergence above the 0°C isotherm in the mature stage of thunderstorm development noted in the Thunderstorm Project (Byers and Braham 1949) and more recently in Doppler radar observations, including those reported here for tropical hot towers (Williams et al. 1991). According to the continuity equation, the horizontal convergence is given by the

vertical gradient of the expression for  $W_i$  in (12). This effect could easily explain the pronounced pregnancy in the convergence profile between the 4.5- and 6.5-km altitudes shown in Fig. 25 of Byers and Braham (1949) for Florida thunderstorms.

In the case of severe storms in highly sheared environments (which are more prevalent at midlatitude than in the tropics), the inclusion of ice in buoyancy calculations may be essential to resolve apparent violations of energy conservation in published observations (Vonnegut and Moore 1958; Roach 1967; Ludlam 1980). In all these studies, the positive area on a tephigram, represented by Eq. (1) and calculated on the basis of the pseudoadiabatic assumption [Eq. (2)], was found to be smaller than the estimated negative area above (bounded by the LNB and the observed overshooting cloud top). The comparisons in Fig. 1 make it clear that the inclusion of ice in buoyancy calculations will simultaneously increase the positive area and reduce the negative area, thereby eliminating the contradiction presented by the conventional pseudoadiabatic calculations.

It is important to emphasize that none of the three methods for CAPE determination is particularly accurate, given the inadequacies of parcel theory. There is, however, little question that the reversible calculation with ice is more accurate than the reversible cal-

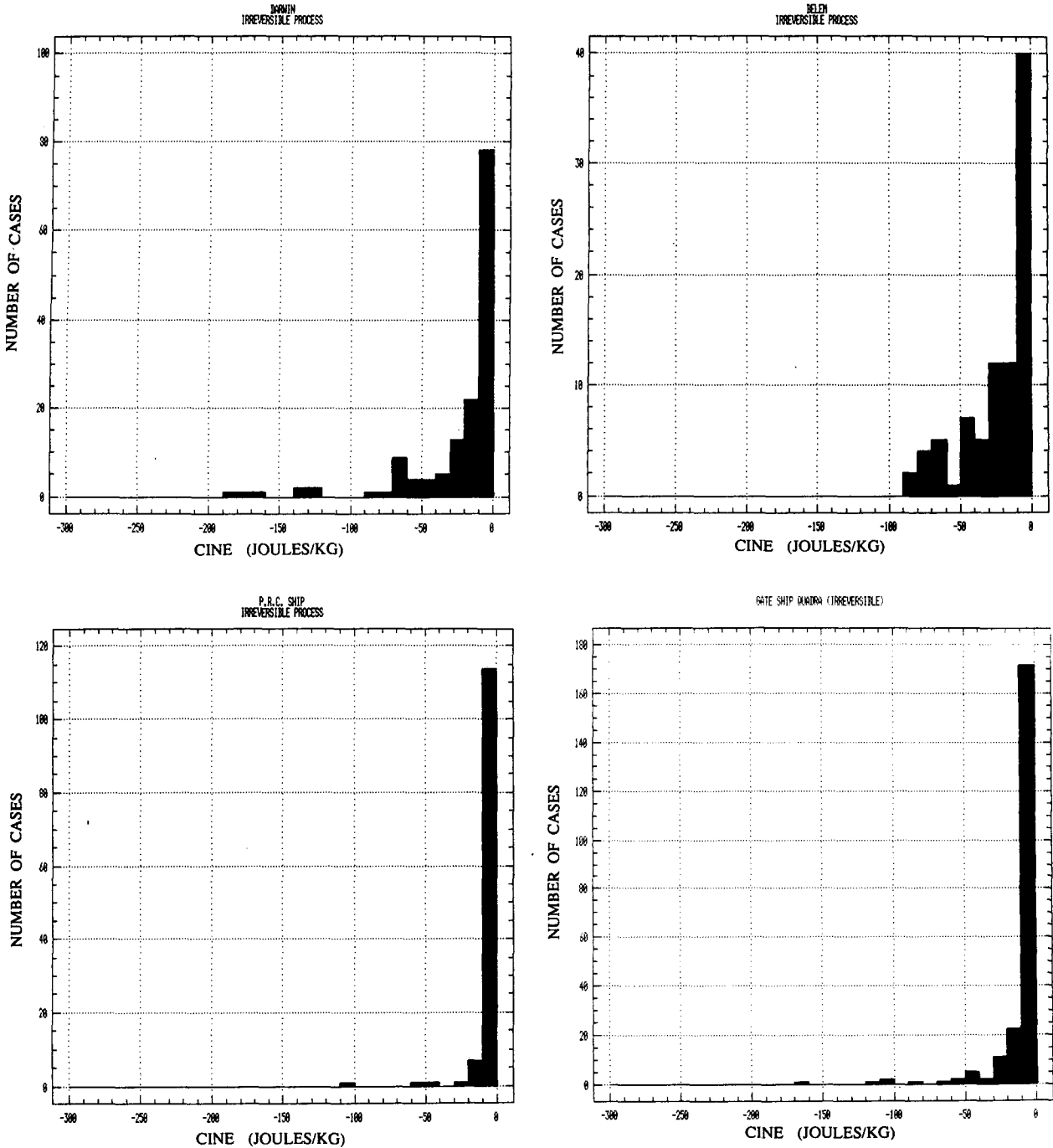


FIG. 8. (a) Histograms of convective inhibition energy (CINE) for (a) Darwin; (b) Belem; (c) PRC ship; (d) *Quadra* ship.

culuation with liquid water loading alone. It may well be unrealistic to carry the adiabatic liquid water content (several grams per cubic meter) to the 200-mb level, for example, but it is even more unrealistic to prevent this water from freezing. As shown in earlier sections, the CAPE calculations with ice lend an unequivocal "yes" to the question posed in the title of Xu and Emanuel (1989) for large regions of the tropical atmosphere.

It is often stated that the tropical atmosphere is close to a condition of moist neutrality. What then does "close" mean? The results of this study, like previous results, show that the tropical atmosphere is substantially closer to a moist neutral condition than a dry neutral one. It is precisely this circumstance that gives the inclusion of the ice phase (vapor deposition and freezing) a far greater influence on CAPE than the 12% latent heat of fusion relative to the latent heat of con-

denensation. When the ice phase is included in the calculations, we have shown that the parcel-theory predictions for velocity appear to account easily for measured velocities. To the extent that vertical motions are attributable to the release of conditional instability in the tropics, it must be concluded that the tropical atmosphere exhibits distinct departures from moist neutrality.

#### *b. Threshold temperatures in the tropical atmosphere*

The CAPE calculations for a variety of locations in the tropics show reasonably well-defined empirical thresholds in the wet-bulb potential temperature. Zero-CAPE intercepts summarized in Table 1 are somewhat dependent on method of CAPE calculation, but all results are close to  $\theta_{wc} = 22^\circ\text{--}23^\circ\text{C}$ . For consistency, all calculations in Table 1 are based on the assumption of lifting from the surface, and it is noteworthy that this assumption leads to a near-zero-CAPE atmosphere over the central oceans, in agreement with Emanuel (1988). For tropical boundary layers with  $\theta_w$  values larger than  $23^\circ\text{C}$ , CAPE increases (on average) at a rate of about  $1000 \text{ J kg}^{-1} \text{ }^\circ\text{C}^{-1}$  of  $\theta_w$ .

Betts and Ridgway (1989) have also observed an "equilibrium" value for boundary layer  $\theta_e$  (347–350 K) in agreement with the  $\theta_{wc}$  values shown in Table 1. It is important to note, based on the results in Fig. 4, that all tropical stations analyzed in this study show systematic increases in CAPE for  $\theta_w$  values larger than the equilibrium  $\theta_{wc}$ , suggesting that tropical convection is generally unable to maintain an equilibrium zero-CAPE atmosphere. The sustained presence of finite CAPE, both day and night over tropical continental regions, is supported by the calculations shown in Fig. 6 and the existence of lightning activity at midnight (Orville and Henderson 1986).

The  $\theta_w$  threshold for finite CAPE is evidently linked with a widely recognized empirical threshold for tropical cyclone formation. As noted earlier, the  $\theta_w$  climatology in Fig. 5 shows that  $\theta_w \geq 23^\circ\text{C}$  in regions over the oceans where such storms originate (Gray 1968). Longstanding evidence is available for a  $26^\circ\text{--}26.5^\circ\text{C}$  threshold in sea surface temperature for the formation of tropical cyclones (Palmen 1948; Anthes 1982; Evans 1991). If the latter temperature threshold is adjusted for the tropical air–sea temperature difference of  $0.5^\circ\text{--}1.0^\circ\text{C}$  (Bottomley et al. 1990) and the 80% relative humidity typical of oceanic boundary-layer air (Riehl 1954), a  $\theta_w$  close to  $\theta_{wc}$  value =  $23^\circ\text{C}$  results. These results taken together suggest that finite CAPE is present prior to tropical cyclone (hurricane) formation and raise questions about the representativeness of numerical formulations that produce hurricanes (Rotunno and Emanuel 1987) without preexisting CAPE.

Several studies (Kotaki and Katoh 1983; Orville and Henderson 1986) show that the lightning activity over the tropical ocean is an order of magnitude less frequent than over the land. Williams et al. (1992) suggest a

quantitative explanation based on the nonlinear dependence of graupel formation on  $\theta_w$  and CAPE. When lightning does occur over the tropical ocean, it is most prevalent over the warmer western regions of the Atlantic and Pacific (where  $\theta_w$  values in Fig. 5 are elevated), often in association with tropical cyclones (Dean 1929; Sashoff 1939; Kimpfara 1958; Black et al. 1986; Venne et al. 1989). Based on evidence for a well-defined threshold for CAPE and an empirical threshold for lightning over the tropical oceans, it is tempting to argue that CAPE is essential for lightning. While this may well be true, at least one argument to the contrary has been posted (Williams 1991).

Other observational studies of convection in the tropical atmosphere have also shown evidence for a threshold temperature. For example, Graham and Barnett (1987) found a dramatic change in convection regimes for a critical SST of  $27.5^\circ\text{C}$ . Raval and Ramanathan (1989) and Stephens and Greenwald (1991) have examined the SST dependence of a greenhouse parameter (essentially the measured difference between the longwave radiation to space and the outgoing longwave radiation from the sea surface). Both studies find a well-defined nonlinear increase in greenhouse parameter for an SST  $\geq 25^\circ\text{--}26^\circ\text{C}$ . On the basis of the results in this paper, we suggest that the onset condition in temperature for conditional instability over tropical oceans has a marked effect on tropical convection.

#### *c. Barriers to the deep release of conditional instability*

The results of this paper support the status quo: large areas in the tropics have significant stored energy available for convection. By "significant," we mean CAPE values sufficient to account for observed vertical velocities in deep tropical convection, according to Eq. (12). Diurnal heating and the low heat capacity of land areas cause maximum CAPE values there, but observations in this study (e.g., Fig. 6) suggest that finite CAPE is present over land and ocean, day and night. The reasons for the substantial discrepancy with other results (Emanuel 1988, 1989; Xu and Emanuel 1989) were discussed in section 6a. The maps of wet-bulb potential temperature in Fig. 5 suggest that more than half of the area within the tropical belt is conditionally unstable. This status quo result again raises the question posed several times in earlier studies (e.g., Byers 1951): Why is the convecting area such a small fraction of the conditionally unstable area?

Energy arguments for moist convection (Bjerknes 1938) predict a small area of ascent and a large area of subsidence, but this steady-state argument does not explain why the initiation of conditional instability is prevented when energy is available, and other barriers to deep convection may be present. Pronounced capping inversions, similar to ones observed in soundings over the North American Great Plains in the spring-

time, are occasionally observed in tropical soundings. In Darwin, Australia, for example, pronounced caps on about 10 days in two wet seasons prevented all deep convection and the appearance of radar echoes, and the CAPE values peaked at 4000–6000 J kg<sup>-1</sup>. Most of the time, however, the temperature inversions are more subtle and daily convection is common, though still occupies a small fractional area (Fig. 7).

Calculations of CINE discussed in section 5 for a number of stations show that on about half the occasions CINE is 20 J kg<sup>-1</sup> or larger, values sufficient to prevent vigorous 6 m s<sup>-1</sup> boundary-layer thermals from achieving the “condition” of conditional instability. Observation of vertical velocities in dry boundary-layer convection suggest that such thermals are relatively rare events (Lenschow and Stephens 1980; Raymond and Wilkening 1982). Other calculations of CINE from tropical soundings (Keenan et al. 1990) show average values significantly larger than 20 J kg<sup>-1</sup>.

Some tropical soundings show no capping inversion, no measureable CINE, but substantial CAPE, and still deep convection breaks out infrequently. Visual observations on such occasions often show the presence of large numbers of shallow cumuli with bases at the LCL that have ceased growing and appear to be neutrally buoyant “fossils.” These observations suggest that the small clouds, which are most susceptible to mixing, ingest dryer environmental air and by evaporative cooling quickly lose the buoyancy they acquire above the level of free convection, thereby preventing them from tapping the stored energy at higher levels. The evaporation cooling also produces penetrative downdrafts that may stabilize the planetary boundary layer.

This study provides only a partial answer to the question posed at the beginning of this section. Further detailed analyses of the soundings and the behavior of clouds that develop in response to these soundings will be necessary to clarify the nature of barriers to the release of conditional instability.

#### *d. Significance of results on conditional instability for general circulation models*

Global variations in boundary-layer moist entropy (as quantified in this study by wet-bulb potential temperature) and consequently CAPE, particularly the land–ocean contrast in these parameters, appear to be mirrored in a number of other meteorological variables, as discussed briefly in section 4. The larger  $\theta_w$  values over continental regions lead to larger vertical velocities (Williams et al. 1991), deeper clouds (Suskind et al. 1984), larger albedo (Harrison et al. 1990), larger transports of ice particles to upper levels of the troposphere (Chiou et al. 1990), substantially more lightning activity (Kotaki and Katoh 1983; Orville and Henderson 1986), larger concentrations of water vapor (Newell et al. 1972) at upper levels, and a reduction in outgoing longwave radiation (Bess et al. 1989) relative to the regions over colder ocean water. All these characteristics are determined essentially by the upward

transport of ice particles in deep tropical convection, a transport that is strongly influenced by CAPE and the moist entropy of the planetary boundary layer emphasized in earlier sections. There is considerable evidence that lightning activity, for example, is dependent on the freezing of supercooled water as rime-on-graupel particles in the mixed-phase region ( $0^\circ \leq T \leq -40^\circ\text{C}$ ) (Williams 1989). Other characteristics of the tropical atmosphere—albedo, outgoing longwave radiation, and upper-level water vapor—depend on small ice particles whose residence times in the upper troposphere (by virtue of their small terminal velocities) range from hours to days. The emplacement of these small ice particles in the upper troposphere of the tropical atmosphere may likely depend on a process that is closer to reversible than processes at lower levels of deep convection. In section 3, the departures from reality in both the reversible and pseudoadiabatic process at lower levels were emphasized. It is possible that the reversible process is a more accurate description for the evolution of ice condensate in the cold ( $T < -40^\circ\text{C}$ ) portions of deep updrafts, where supercooled water is nonexistent and where precipitation formation and efficient removal of the ice by gravitational sedimentation is not possible. If this argument is valid, the  $-40^\circ\text{C}$  level (11–12 km MSL) is of considerable importance in the tropical atmosphere. Analysis of soundings in this study shows that the level of neutral buoyancy is usually above the  $-40^\circ\text{C}$  isotherm, and that this level increases with  $\theta_w$  and CAPE. The substantial land–ocean contrast in the previously mentioned ice-controlled characteristics is probably explicable in terms of differences in  $\theta_w$  as shown in the global climatology in Fig. 5.

In GCMs, the characteristics and parameters cited previously are strongly impacted by cumulus parameterization schemes. The various cumulus parameterization schemes now in use can be distinguished on the basis of how they process CAPE in the atmosphere, or how pervasively boundary-layer air of high  $\theta_w$  is transported to upper levels of the troposphere by moist convection. In light of the results in this study, an important test of how well these schemes process CAPE is how well the GCM results for surface wet-bulb potential temperature agree with the global distributions shown in Fig. 5 and with the observation in Table 1. We are presently seeking GCM results on  $\theta_w$  to make such comparisons for the various cumulus parameterization schemes in current use.

## 7. Conclusions

Conditional instability has been examined for the tropical atmosphere based on thermodynamic, radar, and electrical observations. CAPE has been calculated by three methods (pseudoadiabatic, reversible, reversible with ice). The expectation that ice will dominate the mixed-phase region and will be the sole form of condensate at higher levels of tropical convection suggests that the most accurate parcel-theory calculation

is the reversible-with-ice method, in which it is found that the negative buoyancy of condensate loading is roughly offset by the positive buoyancy from the latent heat of freezing. At all sites examined, CAPE is well correlated with boundary-layer wet-bulb potential temperature, with a well-defined zero-CAPE intercept near 22°–23°C. Global distributions of  $\theta_w$ , a variable that appears to be a reliable proxy for CAPE, show maximum values (23°–28°) over continents, intermediate values over warm ocean water (24°–25°), and values near the zero-CAPE intercept (22°–23°C) over the central Atlantic and Pacific oceans. CINE provides only a partial explanation for the simultaneous presence of widespread CAPE and infrequent deep convection.

*Acknowledgments.* We appreciate assistance and discussion of this topic from Eric (Dr. CAPE) Rasmussen, Tom Keenan, Steve Rutledge, and Kerry Emanuel. We also thank Conrad Ziegler and an anonymous reviewer for helpful comments on the manuscript. The DUNDEE program was supported by the National Science Foundation Grant ATM-8818695, with the assistance and encouragement of R. Taylor. Thermodynamic soundings were generously provided by T. Keenan (AMEX), C. Nobre (ABLE), and D. Joseph and R. Jenne (GATE).

## REFERENCES

- Anthes, R. A., 1982: Tropical cyclones—Their evolution, structure and effects. *Meteor. Monogr.*, **19**, No. 41.
- Bannon, J. K., and L. P. Steele, 1957: Average water-vapor content of the air. Meteorological Research Committee, London, M. R. P. No. 1075, 208 pp.
- Bess, T. S., G. L. Smith, and T. P. Charlock, 1989: A ten-year monthly data set of outgoing longwave radiation from *Nimbus-6* and *Nimbus-7* satellites. *Bull. Amer. Meteor. Soc.*, **70**, 480–489.
- Betts, A. K., 1982: Saturation point analysis of moist convective overturning. *J. Atmos. Sci.*, **39**, 1484–1505.
- , and W. Ridgway, 1989: Climatic equilibrium of the atmospheric convective boundary layer over a tropical ocean. *J. Atmos. Sci.*, **46**, 2621–2641.
- Black, P. G., R. A. Black, J. Hallett, and W. A. Lyons, 1986: Electrical activity of the hurricane. Preprints, *23rd Conf. on Radar Meteorology and Conf. on Cloud Physics*, Snowmass, Colorado, Amer. Meteor. Soc., J277–J280.
- Bluestein, H. B., E. W. McCaul, Jr., G. P. Bird, G. R. Woodall, G. Martin, and S. Keighton, 1989: Mobile sounding observations of a thunderstorm near the dryline: The Gruver, Texas storm complex of 25 May 1987. *Mon. Wea. Rev.*, **117**, 244–250.
- Bottomley, M., C. K. Folland, J. Hsiung, R. E. Newell, and D. E. Parker, 1990: *Global Ocean Surface Temperature Atlas*. Met. Office and MIT, 20 pp.
- Bjerknes, J., 1938: Saturated-adiabatic ascent of air through a dry-adiabatic descending environment. *Quart. J. Roy. Meteor. Soc.*, **64**, 325–330.
- Byers, H. R., 1951: Thunderstorms. *Compendium of Meteorology*, T. E. Malone, Ed., 681–693.
- , and R. B. Braham, 1949: *The Thunderstorm*. U.S. Govt. Printing Office, Washington, D.C.
- Chappell, C. F., and D. R. Smith, 1975: Generation of available buoyant energy by cloud glaciation. *PAGEOPHYS.*, **113**, 825–836.
- Chiou, E. W., M. P. McCormick, W. P. Chu, and G. K. Yue, 1990: Global distributions of cirrus determined from SAGE II occultation measurements between November 1984 and October 1988. Preprints, *Conf. on Cloud Physics*, San Francisco, Amer. Meteor. Soc., 513–517.
- Dean, S. W., 1929: Correlation of directional observations of atmospheric with weather phenomena. *Proc., Inst. Radio Eng.*, **17**, 1185–1191.
- Emanuel, K., 1988: Toward a general theory for hurricanes. *Amer. Sci.*, **76**, 370–379.
- , 1989: Dynamical theories of tropical convection. *Aust. Meteor. Mag.*, **37**, 3–10.
- Evans, J. L., 1991: Tropical cyclone sensitivity to sea surface temperature. *19th Conf. on Hurricanes and Tropical Meteorology*, Miami, Amer. Meteor. Soc., 471–477.
- Gamache, J. F., 1990: Microphysical observations in summer MONEX convective and stratiform clouds. *Mon. Wea. Rev.*, **118**, 1238–1249.
- Garstang, M., S. Ulanski, S. Greco, J. Scala, R. Swap, D. Fitzjarralk, D. Martin, E. Browell, M. Shipman, V. Connors, R. Harris, and R. Talbot, 1990: The Amazon Boundary-Layer Experiment (ABLE 2B): A meteorological perspective. *Bull. Amer. Meteor. Soc.*, **71**, 19–32.
- Graham, N., and T. P. Barnett, 1987: Observations of sea surface temperature and convection over tropical oceans. *Science*, **238**, 657–659.
- Gray, W. M., 1968: Global view of the origin of tropical disturbances and storms. *Mon. Wea. Rev.*, **96**, 669–700.
- Harrison, E. F., P. Minnis, B. R. Barkstrom, V. Ramanathan, R. D. Cess, and G. G. Gibson, 1990: Seasonal variation of cloud radiative forcing derived from the Earth Radiation Budget Experiment. *J. Geophys. Res.*, **95**, 18 687–18 703.
- Iribarne, J. V., and W. L. Godson, 1981: *Atmospheric Thermodynamics*, D. Reidel, 259 pp.
- Keenan, T. D., B. R. Morton, X. S. Zhang, and K. Nguyen, 1990: Some characteristics of thunderstorms over Bathurst and Melville Islands near Darwin, Australia. *Quart. J. Roy. Meteor. Soc.*, **116**, 1153–1172.
- Kimpara, A., 1958: Atmospherics in the Far East. *Recent Advances in Atmospheric Electricity*, L. G. Smith, Ed., Pergamon Press, 565–581.
- Kingsmill, D. E., R. M. Wakimoto, and W.-C. Lee, 1989: Kinematic and dynamic analysis of a microburst producing thunderstorm. Preprints, *24th Conf. on Radar Meteorology*, Tallahassee, Florida, Amer. Meteor. Soc., 146–149.
- Kotaki, M., and C. Katoh, 1983: The global distribution of thunderstorm activity observed by the Ionsphere Sounding Satellite (ISS-b). *J. Atmos. Terr. Phys.*, **45**, 833–847.
- Lemone, M. A., and E. J. Zipser, 1980: Cumulonimbus vertical velocity events in GATE. Part I: Diameter, intensity and mass flux. *J. Atmos. Sci.*, **37**, 2444–2457.
- Lenschow, D. H., and P. L. Stephens, 1980: The role of thermals in the convective boundary layer. *Bound. Layer Meteor.*, **19**, 509–532.
- Ludlam, F. H., 1980: *Clouds and Storms: The behavior and effect of water in the atmosphere*. Pennsylvania State University Press, 405 pp.
- Margules, M., 1905: Über die energie der stürme. *Zentr. Anst. Meteor. Wien*, **40**, 1–26.
- Markson, R., 1986: Tropical convection, ionospheric potentials, and global circuit variation. *Nature*, **320**, 588–594.
- McDonald, J. E., 1963: Early developments in the theory of the saturated adiabatic process. *Bull. Amer. Meteor. Soc.*, **44**, 203–211.
- Moncrieff, M. W., and M. J. Miller, 1976: The dynamics and simulation of tropical cumulonimbus and squall lines. *Quart. J. Roy. Meteor. Soc.*, **102**, 373–394.
- Newell, R. E., J. W. Kidson, D. G. Vincent, and G. J. Boer, 1972: *The General Circulation of the Tropical Atmosphere and Interaction with Extratropical Latitudes*, Vol. 2, MIT Press, 371 pp.
- Orville, R. E., and R. W. Henderson, 1986: Global distribution of midnight lightning: September 1977 to August 1978. *Mon. Wea. Rev.*, **114**, 2640–2653.
- Palmen, E., 1948: On the formation and structure of tropical hurricanes. *Geophysica*, **3**, 26–38.

- Raval, A., and V. Ramanathan, 1989: Observational determination of the greenhouse effect. *Nature*, **342**, 785–761.
- Raymond, D. J., and M. H. Wilkening, 1982: Flow and mixing in New Mexico cumuli. *J. Atmos. Sci.*, **39**, 2211–2228.
- Riehl, H., 1954: *Tropical Meteorology*. McGraw Hill.
- Roach, W. T., 1967: On the nature of the summit areas of severe storms in Oklahoma. *Quart. J. Roy. Meteor. Soc.*, **93**, 318–336.
- Rotunno, R., and K. Emanuel, 1987: An air–sea interaction theory for tropical cyclones. Part II: Evolutionary study using a non-hydrostatic axisymmetric numerical model. *J. Atmos. Sci.*, **44**, 542.
- Rutledge, S., E. R. Williams, and T. Keenan, 1992: The Down Under Doppler and Electricity Experiment (DUNDEE): Overview and Preliminary Results. *Bull. Amer. Meteor. Soc.*, **73**, 3–16.
- Sashoff, S. P., 1939: Static emanating from six tropical storms and its use in locating the position of the disturbance. *Proc., Inst. Radio Eng.*, 696–700.
- Saunders, P. M., 1957: The thermodynamics of saturated air: A contribution to the classical theory. *Quart. J. Roy. Meteor. Soc.*, **83**, 342–350.
- Stephens, G. L., and T. J. Greenwald, 1991: Observations of the Earth's radiation budget in relation to atmospheric hydrology. Part II: Cloud effects and cloud feedback. *J. Geophys. Res.*, **96**, 15 325–15 340.
- Susskind, J., J. Rosenfeld, and D. Reuter, 1984: Remote sensing of weather and climate parameters from HIRSZ/MSV on TIROS-N. *J. Geophys. Res.*, **89**, 4677–4697.
- Venne, M. G., W. A. Lyons, C. S. Keen, P. G. Black, and R. C. Gentry, 1989: Explosive supercell growth: A possible indicator for tropical storm intensification. Preprints, *24th Conf. on Radar Meteorology*, Tallahassee, Florida, Amer. Meteor. Soc., **545–548**.
- Vonnegut, B., and C. B. Moore, 1958: Giant electrical storms. *Recent Advances in Atmospheric Electricity*, L. G. Smith, Ed., Pergamon, 631 pp.
- Williams, E. R., 1989: The tripole structure of thunderstorms. *J. Geophys. Res.*, **94**, 13 151–13 167.
- , 1991: Comments on “Thunderstorms above frontal surfaces in environments with positive CAPE. Part I: A climatology,” *Mon. Wea. Rev.*, **119**, 2511–2513.
- , S. G. Geotis, N. Renno, S. A. Rutledge, E. Rasmussen, and T. Rickenback, 1992: A radar and electrical study of tropical “hot towers.” *J. Atmos. Sci.*, **49**, 1386–1395.
- Williams, E. R., 1992: The Schumann resonance: A global tropical thermometer. *Science*, **256**, 1184–1187.
- Xu, K., and K. A. Emanuel, 1989: Is the tropical atmosphere conditionally unstable? *Mon. Wea. Rev.*, **117**, 1471–1479.
- Zipser, E. J., and R. C. Taylor, 1968: A catalogue of meteorological data obtained during the Line Islands Experiment, February–April 1967. NCAR Tech. Notes, NCAR-TN-35.